

Supplemental experimental procedures

Indirect calorimetry

EE was quantified by indirect calorimetry. This was an open circuit, ventilated hood system (Parvo Medics' TrueOne® 2400, Sandy, UT). The monitor was calibrated against standard gases before each study. Subjects rested in a supine position for 20 minutes before measurement commenced. Gas exchange measurements were recorded continuously for 30 minutes with the first 5 minutes discarded in final analysis. Resting EE was calculated using the equations of Ferrannini (Ferrannini, 1988). The mean day-to-day intra-individual coefficient of variation for resting EE at our institute is approximately 4%. Cold-induced thermogenesis (CIT) was calculated by subtracting resting EE at 12°C from resting EE at 27°C.

EE estimation during maximal exercise test

Increase in EE during maximal exercise was calculated by subtracting EE at maximal aerobic capacity ($\text{VO}_{2\text{max}}$) from EE at baseline, which was measured during a 2-minute resting period on the bike before commencement of pedaling. All subjects achieved target heart rates, predicted as $(220 - \text{age})$ beats per minute, during maximal exercise test.

Body composition

Body composition was measured by dual-energy X-ray absorptiometry (Lunar iDXA; GE Healthcare, Madison, WI, USA) on the same morning of cold exposure test.

Core and skin temperature measurements

Core temperature was measured by the ingestible Jonah™ capsule (Mini Mitter/Respironics, Bend, OR), which volunteers swallowed in the morning prior to each test. Skin temperatures were recorded from iButtons® (Maxim, San Jose, CA), which are adhesive temperature data loggers placed over the deltoid, supraclavicular fossae, upper inner arm, dorsum of hand, pectoralis major, anterior thigh and anterior lower leg. All skin sites were located on the left side of the body. Mean skin temperature was calculated using the Ramanathan method (Levin and Sullivan, 1984). The vasoconstrictive response (an indication of vasoconstriction which reduces heat loss in extremities) was estimated by the distal (dorsum of hand) to proximal (inner arm) temperature gradient. The insulative response (an indication of general peripheral to central blood shunting for heat conservation) was calculated by the skin to core temperature gradient. BAT is most abundant in the supraclavicular fossae and situated less than 10mm from skin surface. Previous studies revealed skin temperature over supraclavicular fossae to be higher than skin over muscle during cold exposure and/or meal challenge (Lee et al., 2011; Symonds et al., 2012), suggesting a BAT thermogenic response. We therefore measured skin temperature over the supraclavicular fossae and estimated BAT thermogenic response by calculating the gradient of the mean fossae temperature and temperature over pectoralis major.

Surface electromyography (EMG)

Wireless surface EMG electrodes (Trigno, DelSys Inc, Boston, MA) were placed on the right side of the body over the following muscle groups: upper trapezius, biceps brachii,

pectoralis major and rectus femoris, to objectively measure the intensity of shivering. Volunteers also indicated to investigators whether they experienced any shivering. Subjects were instructed to remain completely stationary to minimize movement artifacts. These muscles have been shown to contribute significantly to total shivering during cold exposure (Bell et al., 1992; Haman et al., 2004a; Ouellet et al., 2012). EMG signals were collected at 2000 Hz and analyzed with the use of custom-designed (RJB) MATLAB algorithms (The Math-works, Natick, MA). Raw signals were filtered using a Butterworth filter with a 45-500 Hz pass band to remove contamination from low frequency motion artifacts, background electrical contamination and unwanted electrocardiographic signals (Brown et al., 2010). Individual muscle shivering intensity was computed from root mean square (RMS) values, constituted from EMG signals received over 50 milliseconds overlapping periods (Haman et al., 2004b). Whole body shivering intensity was estimated by the mean RMS value calculated from the 4 muscle groups. Using weighted means, based on estimated muscle mass, as suggested by previous studies (Bell et al., 1992), did not alter conclusion of analysis. Baseline RMS values were recorded over 30 minutes when subject was enclosed by thermo-blankets infused with water at 27°C [Figure S1A]. Data from first 5 minutes were discarded in analysis. Shivering activity was calculated by subtracting total EMG activity, beginning at the onset of cold exposure (18°C) until end of study (12°C), from baseline value. Fold change of EMG activity from baseline was used in analysis to examine relationship between shivering and hormonal parameters.

Preparation of samples for irisin quantification using Western blot

Irisin is heavily glycosylated in the circulation (Bostrom et al., 2012). We therefore

performed enzymatic deglycosylation prior to immuno-blotting, as previously described (Bostrom et al., 2012). Briefly, albumin/IgG was first removed from serum using the ProteoExtract-kit (CalBiochem, Billerica, MA). Samples were then acidified and peptides extracted using C18 columns (Phoenix Pharmaceuticals, Burlingame, CA), followed by lyophilization to dryness (Savant SPD1010 SpeedVac Concentrator, Hudson, NH). Extracted peptides were reconstituted in deionized water. Two microgram of sample was subsequently deglycosylated using peptide N-glycosidase F (PNGase F) (New England Biolabs, Ipswich, MA) and finally sonicated, boiled and analyzed using western blot against FNDC5 antibody (Abcam, Cambridge, U.K.), which detects both FNDC5 and irisin (Bostrom et al., 2012). Please note: the anti-FNDC5 antibody (ab93373) used in the experiments is no longer available at Abcam. It has been substituted by ab131390. Western blot was carried out following standard procedure and final band intensity of the irisin band (24 kDa) (QL-BG) was quantified using BioPix iQ22.

To determine the specificity of the primary antibody used in quantitative western blotting, equal quantity of serum was separated by electrophoresis on polyacrylamide gel in five different lanes under identical conditions. After protein transfer, the five lanes were cut from the blot and incubated with anti-irisin antibody pre-mixed with increasing quantity of recombinant FNDC5 protein for 12 hours in the following protein:antibody ratios: 0:1, 1:1, 1.5:1, 2:1 and 3:1. Figure 1G shows quenching of the western signal in a dose-dependent manner, thus confirming the specificity of the antibody employed in our experiment.

To further evaluate accuracy of irisin measurement by quantitative western blotting, we repeated irisin measurement in albumin- and immunoglobulin-depleted and deglycosylated samples by ELISA (Phoenix Pharmaceuticals, Burlingame, CA), according to the manufacturer's protocol, which states a minimum detection limit of 1.29 ng/ml and intra- and inter-assay coefficients of variation of <0.2 ng/ml. Figure S1D-F showed individual irisin levels before and after cold exposure, maximal exercise and sub-maximal exercise test, demonstrating a significant rise in irisin level following sub-maximal exercise. The change in irisin levels correlated positively with shivering intensity [Figure 2E]. These results are in agreement with those obtained from western blotting, thus supporting accuracy of our quantification.

Preparation of serum samples for mass spectrometry

Following albumin and immunoglobulin depletion, as described above, glycosylated and deglycosylated serum samples were separated by electrophoresis on a polyacrylamide gel under standard conditions. The gel was stained with Coomassie blue to visualize protein bands. Discrete bands corresponding to molecular weight of FNDC5-immunoreactive bands were excised and digested with trypsin, and the peptides were analyzed by liquid chromatography-tandem mass spectrometry (LC-MS/MS) at the Taplin Mass Spectrometry Facility (Harvard Medical School). The fragmentation patterns of peptide ions were matched to protein sequences by using Sequest.

Other hormone and substrate measurement

Plasma FGF21 was measured by ELISA (BioVendor, Oxford, U.K.), according to the

manufacturer's protocol, with intra-assay and inter-assay coefficients of variation of 3.6% and 3.8%, respectively. Individual FGF21 results are shown in Figure S1G-I. Catecholamines were measured by the laboratories of Eunice Kennedy Shriver, NICHD, and remaining hormonal/substrate tests by NIH Department of Laboratory Medicine.

PET-CT analysis

BAT is defined as tissue with Hounsfield units -300 to -10 on CT (i.e. adipose tissue density) with a standard uptake value of >1.5 (i.e. high glucose uptake signifying high metabolic activity) (Cypess et al., 2009; Saito et al., 2009; van Marken Lichtenbelt et al., 2009; Virtanen et al., 2009). BAT positive status is defined as the presence of >4 ml of tissue satisfying BAT criteria.

Human adipocyte culture

Thermogenic effects of FNDC5 and FGF21 were tested on primary adipocytes established from cervical adipose tissue, a location where BAT precursors are found in humans, obtained during elective thyroid surgery (N=6, age=44 \pm 7, F=4). All patients were euthyroid at time of surgery and provided written informed consent. To determine whether FNDC5/FGF21 impart depot-specific effects, experiments were repeated in adipocyte culture established from omental and subcutaneous fat obtained in 6 adults during elective abdominal surgery or percutaneously under local anesthesia.

Precursors isolated from stromal vascular fraction of adipose tissue were cultured in 75 cm³ flasks until 90% confluence in growth medium, which was DMEM with 10%

newborn calf serum (Invitrogen, Carlsbad, CA), 10 mM HEPES, 33 μ M biotin (Sigma, St. Louis, MO) and 50 U/ml penicillin, and 50 μ g/ml streptomycin. Cells were then trypsinized and plated either in 0.2% gelatin-coated standard 24-well (25×10^4 cells/ well) microplates for RNA isolation, 24-well (5×10^4 cells/well) microplates (Seahorse Bioscience) for cellular respiration experiments, or 96-well (1×10^4 cells/well) microplates for infrared thermography (IRT) studies. Differentiation of adipocytes was undertaken in microplates. Cells were first switched to induction medium, which was growth medium supplemented with 1 μ M dexamethasone (Sigma), 500 μ M 3-isobutyl-1-methylxanthine (Sigma) and 0.85 μ M insulin (Invitrogen, Grand Island, NY) and 1 μ M rosiglitazone (Sigma). After two days, cells were changed to differentiation medium, which was induction medium without dexamethasone but supplemented with 200 μ M indomethacin. Medium was changed every other day during proliferative and differentiative phases until full differentiation.

Adipocyte treatment

After differentiation for 5 days, differentiated adipocytes were treated for 6 days with vehicle (PBS), or 10 or 100 nM recombinant FNDC5 (Abnova, Taipei City 114 Taiwan) and/or recombinant FGF21 protein (Abcam) before IRT study. Adipocytes were treated with vehicle (PBS), or 100nM FNDC5 and/or FGF21, or irisin (Phoenix Pharmaceuticals, Burlingame, CA) in gene/protein expression and cellular respiration experiments. To mimic the effect of cold exposure *in vitro*, adipocytes were incubated in 1 μ M of norepinephrine (Sigma) overnight prior to FGF21 secretory response analysis.

The sequence of recombinant FNDC5 (black), recombinant irisin (underlined), and detected peptide in FNDC5-immunoreactive bands (red) in human serum are shown below:

MPPGPCAWPPRAALRLWLGCVCFALVQADSPSAPVNVTVRHLKANSVVSWD
VLEDEVVIGFAISQQKKDVRMLRFIQEVNTTTRSCALWDLEEDTEYIVHVQAISIQ
GQSPASEPVLFKTPREAEKMASKNKDEVTMKEMGRNQQLRTGEVLIIVVVLFM
WAGVIALFCRQYDIIKDNEPNNNKEKTKSASETSTPEHQGGGLLSKI

Gene and protein expression

RNA concentration/quality was assessed by a NanoDrop spectrophotometer (NanoDrop Technology, Wilmington, DE). For quantification of target gene mRNA levels, reverse-transcription PCR was performed on a GeneAmp PCR System 9700 using the Multiscribe Reverse Transcriptase method (Applied Biosystems, Foster City, CA, USA) with 1 µg of RNA. Real-time quantitative PCR was performed to determine cDNA content in triplicate on a Step One Plus instrument (Applied Biosystems, Foster City, CA) using Taqman Gene Expression assays (Applied Biosystems): *UCP1* (Hs00222452_m1), *PRDM16* (Hs00922674_m1), *PGC1α* (Hs01016719_m1), *CIDEA* (Hs00154455_m1), *DIO2* (Hs00988260_m1), *ZIC1* (Hs00602749_m1), *LHX8*

(Hs00418293_m1), *TBX1* (Hs00271949_m1), *TMEM26* (Hs00415619_m1), *HOXC9* (Hs00396786_m1), *FABP4* (Hs01086177_m1), *PPIA* (Hs04194521_s1).

Relative mRNA levels were calculated by the comparative threshold cycle method using *PPIA* as the housekeeping gene. For Western blotting, protein concentrations were determined using BCA Protein Assay Kit (Thermo Scientific Pierce, Rockford, IL). Twenty microgram of protein fractions were separated by 10% SDS-PAGE, blotted to a nitrocellulose membrane, and detected by rabbit polyclonal anti-human-UCP1 (U6382; Sigma) and mouse monoclonal anti-human-beta-actin (A5316; Sigma).

Reagents in cellular respiration experiments

Mitochondrial function assessment was performed in XF24-3 Extracellular Flux bioanalyzer (Seahorse Bioscience, North Billerica, MA). Adipocytes were incubated in XF-assay medium containing 25 mM glucose, 1mM sodium pyruvate and 2mM GlutMAX. Cells were treated with 1 μ M oligomycin (an ATP synthase inhibitor) and 0.8 μ M FCCP (carbonyl cyanide-p-trifluoromethoxyphenylhydrazone, an ionophore), rendering uncoupled and maximal respiration. Rotenone was added finally to block mitochondrial respiration. For determination of norepinephrine-induced thermogenesis, 1 μ M norepinephrine (Sigma) was injected after baseline measurements. Basal, uncoupled (*i.e.*, oligomycin-insensitive and FCCP-induced maximal) and norepinephrine-induced respiration rates were normalized by total cell protein content per well using BCA Protein Assay Kit (Thermo Scientific Pierce, Rockford, IL). Figure S2B showed a representative plot from one experiment demonstrating sequence of events.

Infrared thermography

Infrared thermography (IRT) was employed to directly measure heat production from cultured adipocytes, as previously described (Lee et al., 2013), which was modeled on a system developed by Paulik and colleagues (Paulik et al., 1998). Adipocytes were differentiated and treated with either vehicle (PBS), FGF21 and/or FNDC5, in a 96-well microplate, as described under *Adipocyte treatment*. To mimic the effect of acute cold exposure, adipocytes were treated with 1 or 10 μ M norepinephrine and then incubated for 10 minutes at 37°C, before measuring real-time thermogenesis. IRT was performed by maintaining temperature of the microplate at 37°C using an insulating system, as shown in Figure S2G. Images were acquired by an infrared camera (FLIR systems 440, Wilsonville, OR), which detects a 7.5-13 μ m spectral response with a thermal sensitivity of $<0.045^{\circ}\text{C}$, and analyzed using the FLIR Quick Report software, available at the manufacturer's website.

Table S1 (Related to Table 1) Correlations between physiologic responses during cold exposure and irisin/FGF21 fold changes. Irisin fold changes were most strongly associated with shivering, among all components of cold-induced thermogenesis (CIT).

		CIT	IR	VR	TR	Shivering	Irisin	FGF21
CIT	Correlation Coefficient	1.000	-.815**	-.184	-.535	.689*	.427	-.797**
	Sig. (2-tailed)	.	.004	.611	.111	.028	.219	.006
	N	10	10	10	10	10	10	10
IR	Correlation Coefficient	-.815**	1.000	-.092	.411	-.320	-.093	.409
	Sig. (2-tailed)	.004	.	.801	.238	.367	.798	.241
	N	10	10	10	10	10	10	10
VR	Correlation Coefficient	-.184	-.092	1.000	.151	-.311	-.307	.339
	Sig. (2-tailed)	.611	.801	.	.678	.382	.389	.337
	N	10	10	10	10	10	10	10
TR	Correlation Coefficient	-.535	.411	.151	1.000	-.004	.251	.772**
	Sig. (2-tailed)	.111	.238	.678	.	.992	.484	.009
	N	10	10	10	10	10	10	10
Shivering	Correlation Coefficient	.689*	-.320	-.311	-.004	1.000	.907**	-.571
	Sig. (2-tailed)	.028	.367	.382	.992	.	.000	.085
	N	10	10	10	10	10	10	10
Irisin	Correlation Coefficient	.427	-.093	-.307	.251	.907**	1.000	-.349
	Sig. (2-tailed)	.219	.798	.389	.484	.001	.	.323
	N	10	10	10	10	10	10	10
FGF21	Correlation Coefficient	-.797**	.409	.339	.772**	-.571	-.349	1.000
	Sig. (2-tailed)	.006	.241	.337	.009	.085	.323	.
	N	10	10	10	10	10	10	10

** . Correlation is significant at the 0.01 level (2-tailed).

* . Correlation is significant at the 0.05 level (2-tailed).

IR = insulative response (body temperature gradient: skin-core)

VR = vasoconstrictive response (body temperature gradient: arm-hand)

TR= thermogenic response (body temperature gradient: supraclavicular fossae-chest)

FGF21=fibroblast growth factor-21

Figure S1 Additional information on clinical experiments (related to Figure 1). Panel A shows clinical setup of cold exposure test. Volunteers rested in a bed in a room at an ambient temperature of 24°C. Two water-infused thermoblankets, one placed on top of and one underneath the individual, allowed rapid and precise adjustment of temperature exposure through altering the temperature of infusing water. Panels B and C are full-sized images of the immunoblots shown in Figure 1C in the main document, from a subject (Subject 1) who shivered [B] and a subject who did not (Subject 2) [C]. The red rectangles represented the cropped portion of the blots displayed in Figure 1C. Panels D-F showed individual changes in deglycosylated irisin and Panels G-I individual FGF21 levels during cold exposure, maximal exercise and submaximal exercise, measured by enzyme immunosorbant assays, * $p < 0.05$ compared with baseline. Data are presented as mean \pm SD.

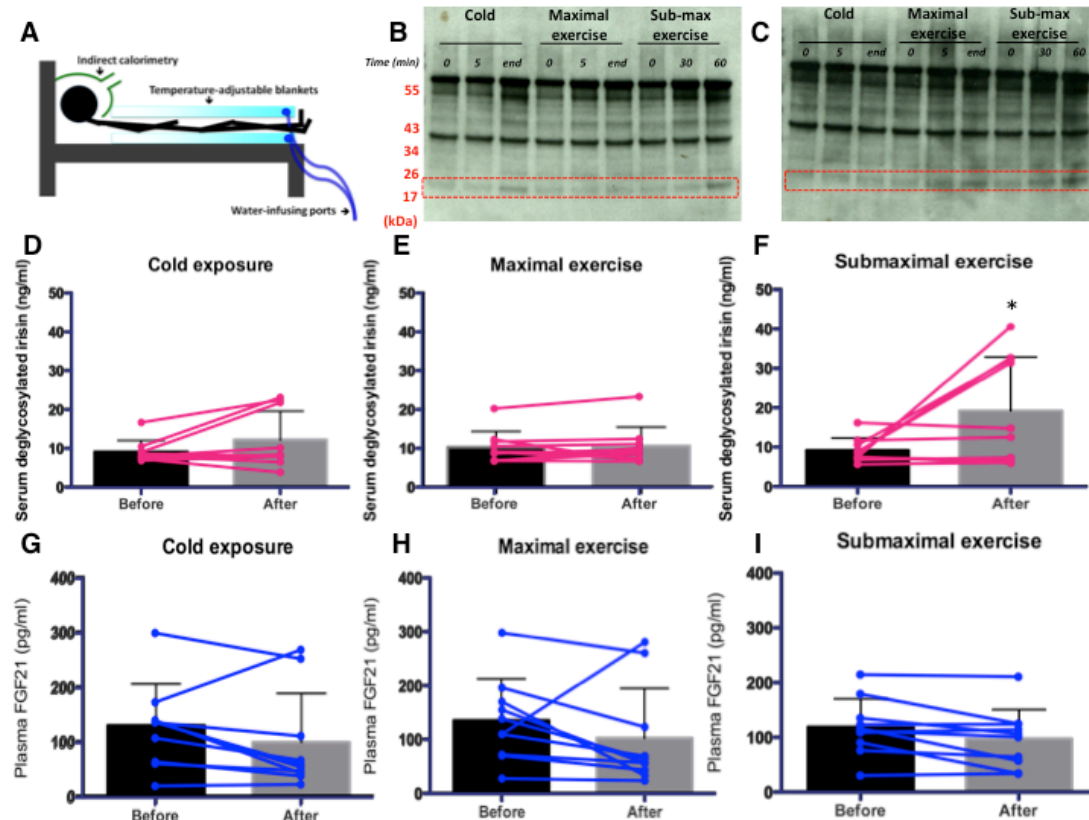


Figure S2 Additional *in vitro* results and methodological details (related to Figure 3).

The “browning” effects of FNDC5 and irisin were similar in neck adipocytes on gene [Panel A] and protein [Panel E] levels. Enhancing effects on basal [Panel C] and uncoupled respiration [Panel D] in adipocytes by FNDC5 and irisin treatment were not statistically different. Panel F showed increase in UCP1 protein levels in subcutaneous adipocytes following FNDC5 and/or FGF21 treatment. Panel B is a representative plot of respiratory uncoupling experiment. Basal oxygen consumption (OCR) was averaged by 4 consecutive measurements recorded in 5 wells. All measurements were shown as percentage changes from baseline OCR. Two forms of uncoupled OCR were measured. Arrow a) indicates the addition of oligomycin, an ATP synthase inhibitor. The nadir represents oligomycin-insensitive uncoupling. Arrow b) indicates addition of the ionophore FCCP while arrow c) indicates addition of rotenone, mitochondrial inhibitor. The difference between the peak OCR induced by FCCP and the trough induced by rotenone equates maximal uncoupling. Both oligomycin-insensitive and maximal uncoupled respiration were increased following FNDC5 and/or FGF21 treatments. Panel G is a schematic diagram of infrared thermography of cultured adipocytes. Adipocytes grown in 96-well microplates were placed on a 37°C heat block in an insulating polystyrene box, lined with black-colored paper to prevent heat radiation. Infrared (IR) camera was placed 30 cm vertically above microplate via an aperture. The distance allowed capturing of central path of heat emission from the centre of the plate, including 4x4 wells, as shown in the bird’s eye view, and represents the analysis window displayed in Figure 2H in **Results**. Data are presented as mean \pm SD.

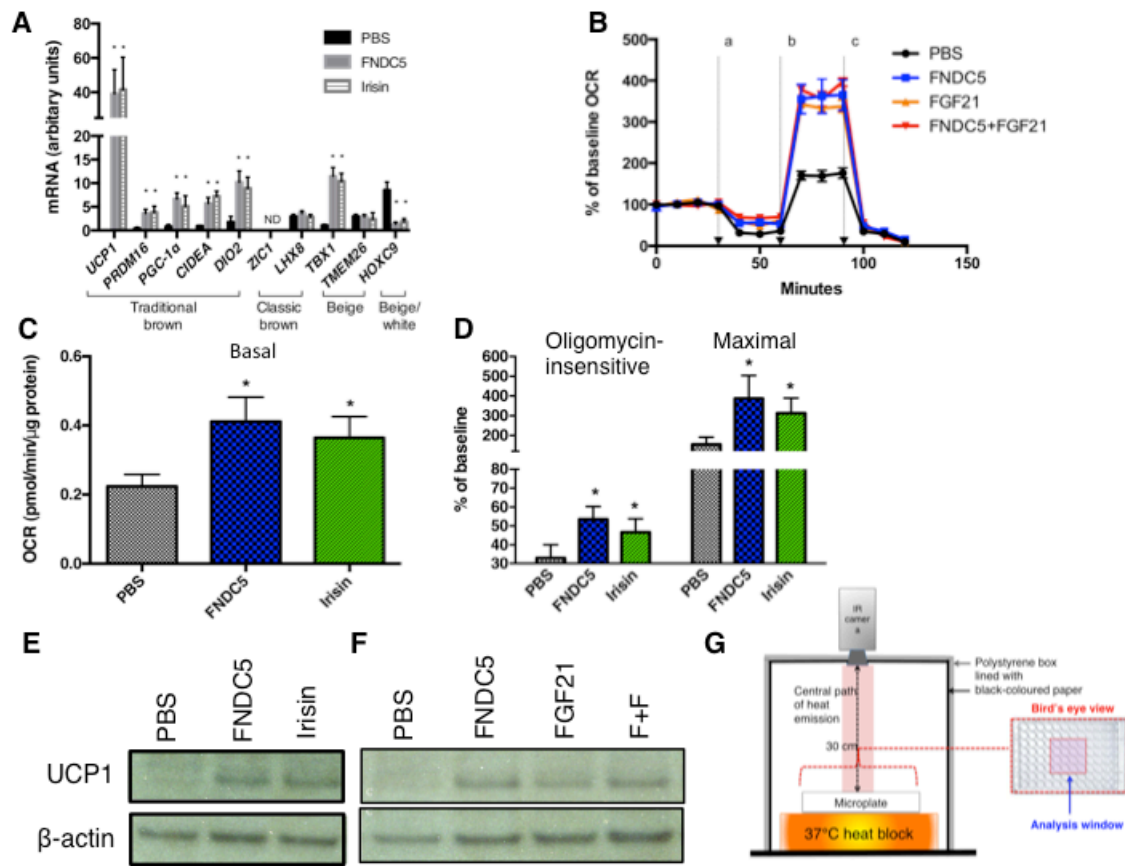
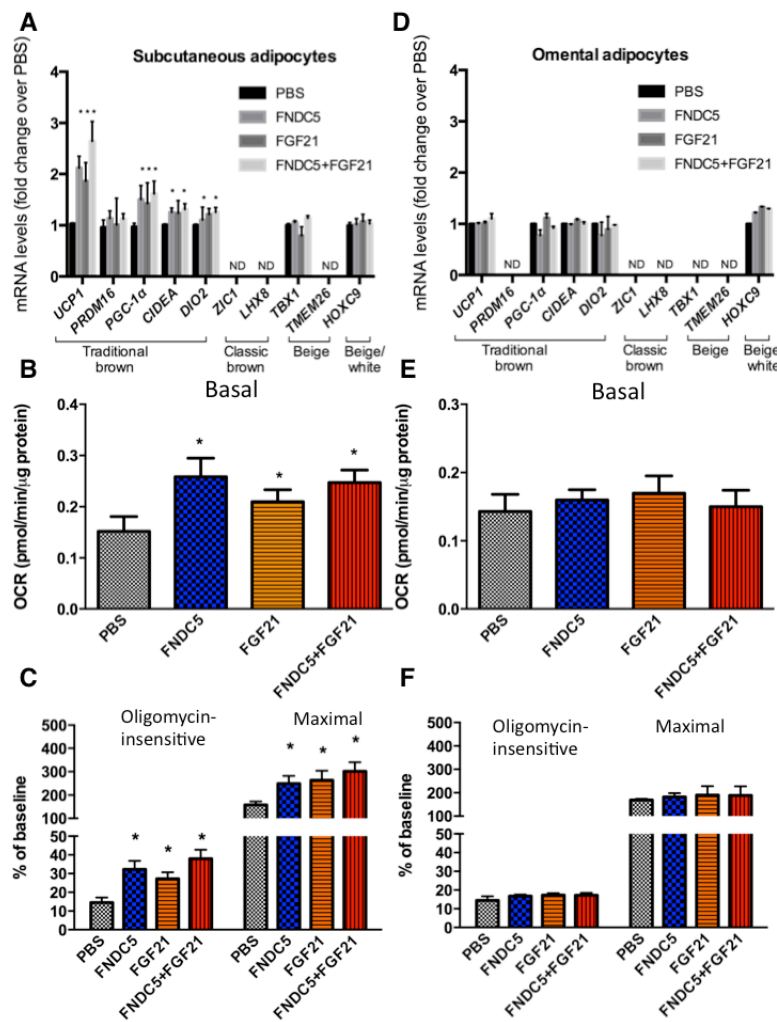


Figure S3 Effects of FNDC5 and/or FGF21 treatment on gene and bioenergetics in subcutaneous and omental adipocytes (related to Figure 3). Effects of FNDC5 and/or FGF21 treatment on brown and beige gene expression [Panel A] and cellular respiration [Panel B and C] in subcutaneous adipocytes. These effects were absent in omental adipocytes [Panels D-F]. The more modest/absent effects of FNDC5/FGF21 on subcutaneous and omental adipocytes, compared to neck adipocytes [Figure 2], could be related to less abundant beige adipocytes in subcutaneous and omental depot, as indicated by lower/absent expression of beige fat gene markers. * $p < 0.05$ compared to baseline. Data are presented as mean \pm SD.



Supplementary References

- Bell, D.G., Tikuisis, P., and Jacobs, I. (1992). Relative intensity of muscular contraction during shivering. *J Appl Physiol* 72, 2336-2342.
- Bostrom, P., Wu, J., Jedrychowski, M.P., Korde, A., Ye, L., Lo, J.C., Rasbach, K.A., Bostrom, E.A., Choi, J.H., Long, J.Z., *et al.* (2012). A PGC1- α -dependent myokine that drives brown-fat-like development of white fat and thermogenesis. *Nature* 481, 463-468.
- Brown, S.H., Brookham, R.L., and Dickerson, C.R. (2010). High-pass filtering surface EMG in an attempt to better represent the signals detected at the intramuscular level. *Muscle Nerve* 41, 234-239.
- Cypess, A.M., Lehman, S., Williams, G., Tal, I., Rodman, D., Goldfine, A.B., Kuo, F.C., Palmer, E.L., Tseng, Y.H., Doria, A., *et al.* (2009). Identification and importance of brown adipose tissue in adult humans. *N Engl J Med* 360, 1509-1517.
- Ferrannini, E. (1988). The theoretical bases of indirect calorimetry: a review. *Metabolism* 37, 287-301.
- Haman, F., Legault, S.R., Rakobowchuk, M., Ducharme, M.B., and Weber, J.M. (2004a). Effects of carbohydrate availability on sustained shivering II. Relating muscle recruitment to fuel selection. *J Appl Physiol* 96, 41-49.
- Haman, F., Peronnet, F., Kenny, G.P., Doucet, E., Massicotte, D., Lavoie, C., and Weber, J.M. (2004b). Effects of carbohydrate availability on sustained shivering I. Oxidation of plasma glucose, muscle glycogen, and proteins. *J Appl Physiol* 96, 32-40.
- Lee, P., Ho, K.K., and Greenfield, J.R. (2011). Hot fat in a cool man: infrared thermography and brown adipose tissue. *Diabetes Obes Metab* 13, 92-93.
- Lee, P., Werner, C.D., Kebebew, E., and Celi, F.S. (2013). Functional thermogenic beige adipogenesis is inducible in human neck fat. *Int J Obes (Lond)*. doi: 10.1038/ijo.2013.82.
- Levin, B.E., and Sullivan, A.C. (1984). Regulation of thermogenesis in obesity. *Int J Obes* 8 Suppl 1, 159-180.
- Ouellet, V., Labbe, S.M., Blondin, D.P., Phoenix, S., Guerin, B., Haman, F., Turcotte, E.E., Richard, D., and Carpentier, A.C. (2012). Brown adipose tissue oxidative metabolism contributes to energy expenditure during acute cold exposure in humans. *J Clin Invest* 122, 545-552.
- Paulik, M.A., Buckholz, R.G., Lancaster, M.E., Dallas, W.S., Hull-Ryde, E.A., Weiel, J.E., and Lenhard, J.M. (1998). Development of infrared imaging to measure thermogenesis in cell culture: thermogenic effects of uncoupling protein-2, troglitazone, and beta-adrenoceptor agonists. *Pharm Res* 15, 944-949.
- Saito, M., Okamatsu-Ogura, Y., Matsushita, M., Watanabe, K., Yoneshiro, T., Nio-Kobayashi, J., Iwanaga, T., Miyagawa, M., Kameya, T., Nakada, K., *et al.* (2009). High incidence of metabolically active brown adipose tissue in healthy adult humans: effects of cold exposure and adiposity. *Diabetes* 58, 1526-1531.
- Symonds, M.E., Henderson, K., Elvidge, L., Bosman, C., Sharkey, D., Perkins, A.C., and Budge, H. (2012). Thermal imaging to assess age-related changes of skin

temperature within the supraclavicular region co-locating with brown adipose tissue in healthy children. *J Pediatr* 161, 892-898.

van Marken Lichtenbelt, W.D., Vanhommerig, J.W., Smulders, N.M., Drossaerts, J.M., Kemerink, G.J., Bouvy, N.D., Schrauwen, P., and Teule, G.J. (2009). Cold-activated brown adipose tissue in healthy men. *N Engl J Med* 360, 1500-1508.

Virtanen, K.A., Lidell, M.E., Orava, J., Heglind, M., Westergren, R., Niemi, T., Taittonen, M., Laine, J., Savisto, N.J., Enerback, S., *et al.* (2009). Functional brown adipose tissue in healthy adults. *N Engl J Med* 360, 1518-1525.